EFFECTS OF SCINTILLATIONS IN GNSS OPERATION

Y. Béniguel, J-P Adam
IEEA, Courbevoie, France

1. Introduction

At altitudes above about 80 km, molecular and atomic constituents of the Earth's atmosphere are energised and ionised by solar ultraviolet (UV) radiation and additionally by energetic electrons of solar and magnetospheric origin in particular at high latitudes. The resulting plasma whose density peaks around 300 km is a dispersive and due to the geomagnetic field also an anisotropic propagation medium for radio waves. The plasma interacts with radio waves to degrade transionospheric propagation at the VHF up to the C-band frequency range.

Whereas medium scale variations in time and space such as Traveling Ionospheric Disturbances (TID's) mainly impact reference networks, local small scale irregularities may cause radio scintillations inducing severe signal degradation and even loss of lock at any user. Amplitude scintillations and phase fluctuations are produced by refractive and diffractive scatter by ionospheric plasma-density irregularities, especially at equatorial and auroral-to-polar latitudes.

The study of this ionosphere variability is one of the aims of the space weather studies for navigation systems. They divide into two kinds of studies: the Total Electron Content (TEC) variability and the scintillations. The TEC is defined as the sum of electrons along a line, usually considered at the zenith of one observation point. Magnetic storms and traveling disturbances may greatly enhance the TEC variability and affect consequently the navigation systems. Intensity of magnetic storms is predominant at high latitudes whereas traveling disturbances mainly occur at mid latitudes.

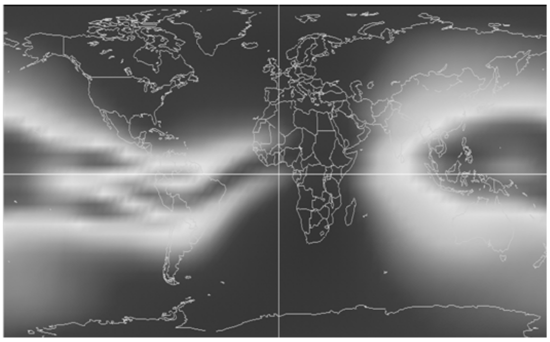

TEC map

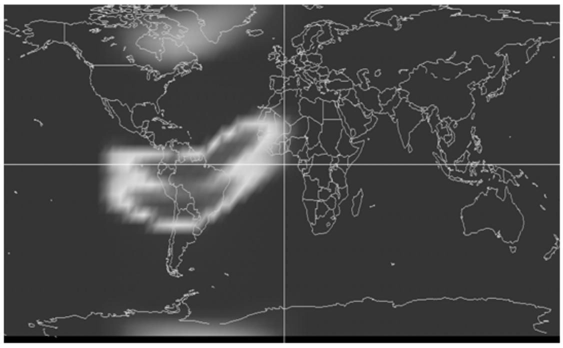

Scintillations map

Figure 1 : TEC and scintillations maps

Geographically, the two areas most affected by scintillations are equatorial (+/- 30 degrees magnetic latitude) and auroral (around the poles) regions. In solar active years - during the peak of the 11-year solar cycle -, both, the diurnal scintillations (occurring in the equatorial region after sunset) as well as the ionospheric-storm induced scintillations can cause significant link outages leading to a degradation of navigation tasks.

<u>Scintillations at equatorial regions</u>

A typical example of scintillations is presented on figure 2. for L1 frequency, both for phase and scintillations. These data have been recorded at Ascencion Island. The scintillations start after sunset. They last in that case approximately one hour. The intensity and phase scintillations are correlated.

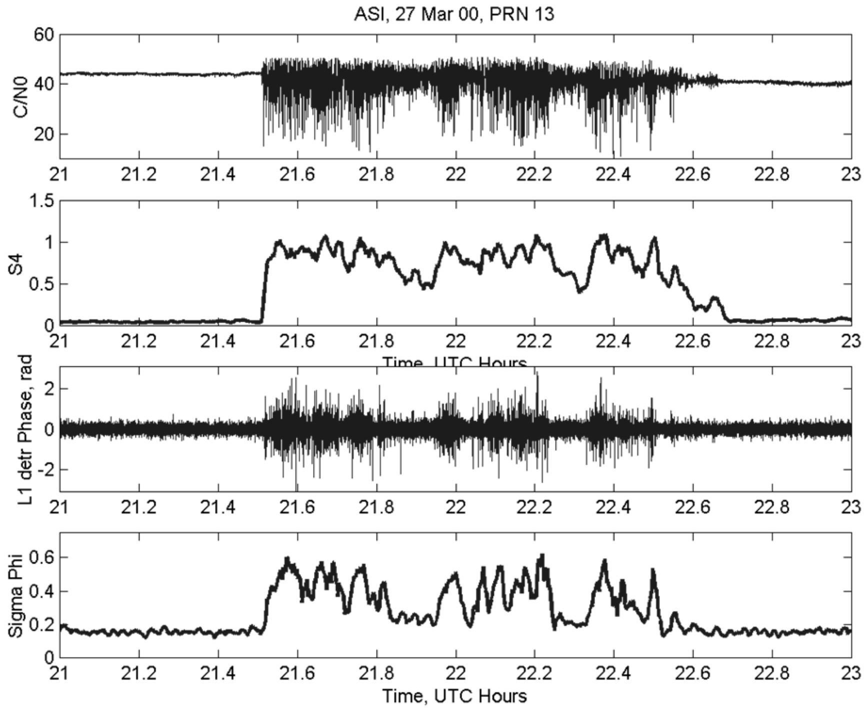

Figure 2: Scintillations recorded at Ascencion Island (Courtesy K. Groves, AFRL)

The figure 3 shows the percentage occurrence of amplitude scintillations in the equatorial zone. The fades amplitude is characterized by the scintillation index S4 which corresponds to the standard deviation of the intensity fluctuations. Its value is between 0 (no scintillation) and 1 (saturated).

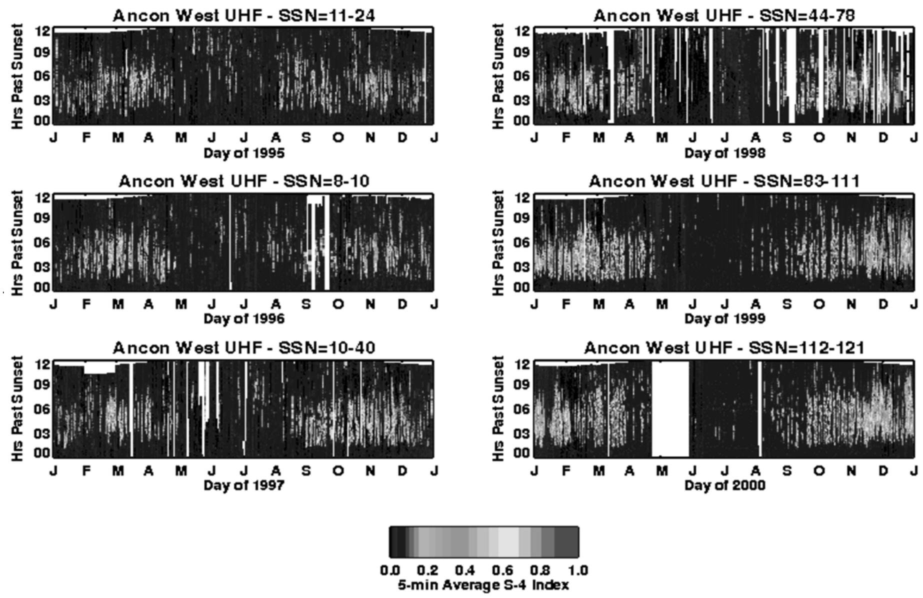

Figure 3: Scintillations dependency on the season and on the solar activity (Courtesy K. Groves, AFRL)

As can be seen from the measurements, the scintillations activity increases with the solar activity (peak value in year 2000). There are typically two periods of the year of higher activity in spring and fall and as shown on the previous figure, the scintillations appear in the post sunset hours and last a few hours.

Polar regions

The polar region extends approximately from magnetic latitude 55° up to the pole. The amplitude scintillations are much lower than in the equatorial case. Typical peak values of the scintillation index are equal to 0.2

Systematic studies of the radio scintillations can help to avoid problems in communication with satellites. Since transionospheric propagation errors due to ionospheric scintillations are a major source of errors in space based communication and navigation, the prediction of ionospheric scintillations is a promising way to reduce the impact of scintillations on operational systems.

Several studies have been already performed showing clear evidences of space weather - induced adverse effects on the Earth's ionosphere-plasmasphere system. Such effects can ultimately cause various types of problems such as range errors, rapid phase and amplitude fluctuations (radio scintillations) of satellite signals, leading to pronounced signal degradation and correspondingly to a degradation of the system performance.

Models are needed in particular to forecast the behavior of modeled ionospheric parameters some hours ahead to ensure high reliability of the Galileo system.

One of these models, the GISM model (ITU model) that has been developed at IEEA [1], allows obtaining the different scintillation parameters, including the generation of time series for Test Cases. Such an example of a time series is given below for the fades amplitude. The slope of the intensity variations can be calculated from these values. The ability of the system to cope with such fluctuations is dependent on this slope variation.

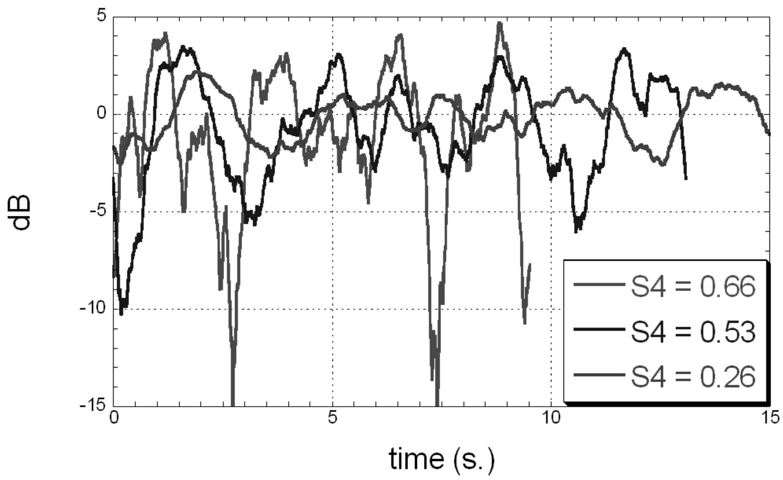

Figure 4: Time series obtained with the GISM scintillation model

As GISM simulations show, the peak to peak dynamics of signal strength may be greater than 20 dB in a strong fluctuations case.

2. Data Analysis

The scintillations are mainly characterized by the S4 and sigma phi parameters which are the standard deviations of the intensity and phase of the signals received. Additional parameters such as the fades amplitudes and durations and their related probabilities are also of interest for system studies. The extent of the scintillation region is of particular interest regarding the probability that a user link can be affected by scintillations. The knowledge of this value is also one objective of the scintillations measurements campaigns.

All these parameters highly depend on the space weather geophysical characteristics: the solar spot number, the magnetic activity (specialy at high latitudes), the latitude, the season and the local time.

The results presented below have been deduced from measurements of GPS signals recorded in Douala, Cameroon and in São Jose dos Campos, Brazil, in the low latitude region. The data in Douala were recorded in 2004 using a GPS scintillation receiver installed by ESA / ESTEC [2], [3]. The data obtained in São Jose dos Campos were recorded in 2002 by INPE, Brazil. The solar flux numbers were respectively equal to 100 in Douala (2004) and 190 in Brazil (2002) in relation with the solar cycle. Both receivers record the data at a 50 Hz sampling frequency. In Douala both intensity and phase of signal received have been analyzed. In São Jose dos Campos, only the intensity has been analyzed.

From 50 Hz raw data, this receiver computes the amplitude and phase scintillation indices S4 and σ_ϕ, which are the standard deviations of the intensity and phase of the received signals. In addition to the GPS satellites, the receiver installed in Douala is able to track the SBAS signal of the EGNOS geostationary satellite PRN 131. It extracts scintillation parameters from this GPS like signal. This is of particular interest due to the fact that only the ionosphere motion modifies the received signal. This satellite is seen with a relatively low elevation angle and the power received is reduced as compared to the GPS satellites.

3. Spatial extent

Since the receiver provides information about the satellite position (azimuth and elevation angles), an analysis of the spatial behaviour of the scintillation activity is possible. Figures 5 and 6 apply to data recorded in Douala. We have considered an arbitrary day: 2004-05-11, between 19 and 20. Figure 5 presents the tracks of the visible satellites. Figure 6 shows the corresponding S4 values recorded.

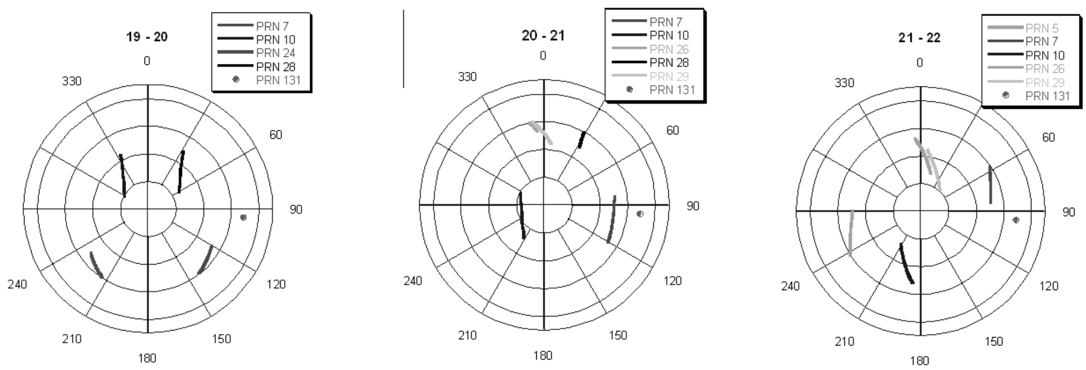

Figure 5 : Visible GPS satellites on 2004-05-11. Elevation vs. azimuth is represented for 3 hours between 19 and 22. All Satellites over 30° were taken into account.

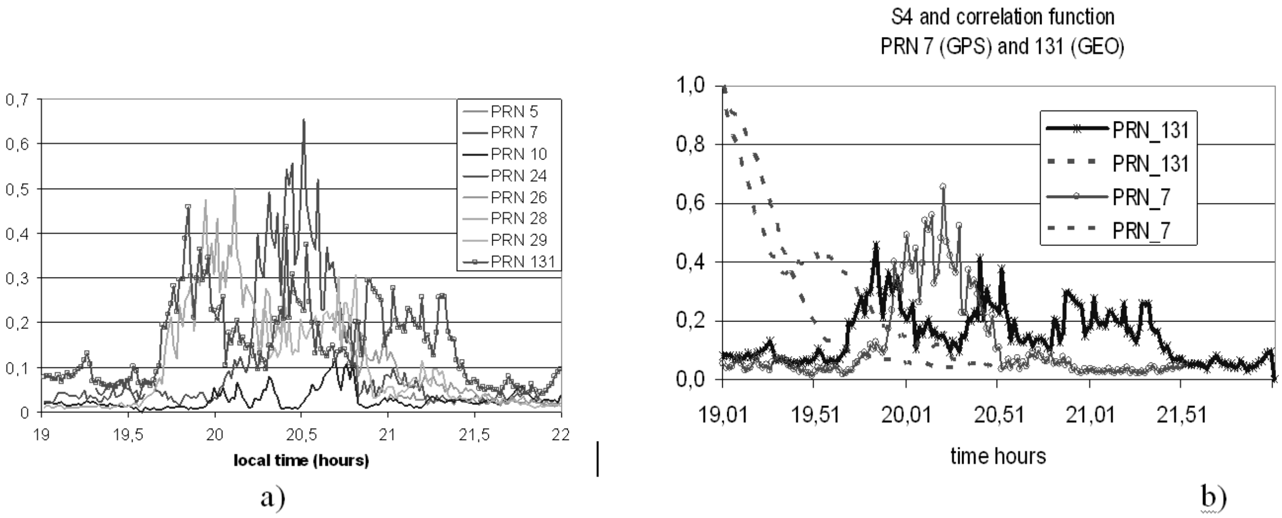

Figure 6: S4 recorded for each satellite visible on 2004-05-11 between 19 and 22 (a) and correlation function (b).

For this period, the GEO satellite link recorded a scintillation activity (Figure 6 a). The GPS satellites PRN 28 and PRN 7 coming near the angular position of the GEO satellite also experienced high scintillation activity. In addition, PRN 29 and PRN 26 were at intermediate distance from PRN 131 and were also affected by moderate scintillation activity. On the contrary, PRN 24, PRN 10 and PRN 5 weren't affected by scintillation.

The duration of scintillations is typically of the order of 1 hour. Calculations of correlation distances have been performed separately and are presented on Figure 6 b. The correlation time which can be deduced is approximately 15 minutes (about 4° of earth rotation). At the altitude of the F-layer, set to 300 km for this example, it would correspond to an inhomogeneities region of about 450 km of diameter. For an observation point on the earth surface the separation angle is 72° for the worst geometrical location.

The same calculations were made from data at São Jose dos Campos (flux number 190). The results obtained are presented on Figure 7. The average extent is about 40 minutes in that case.

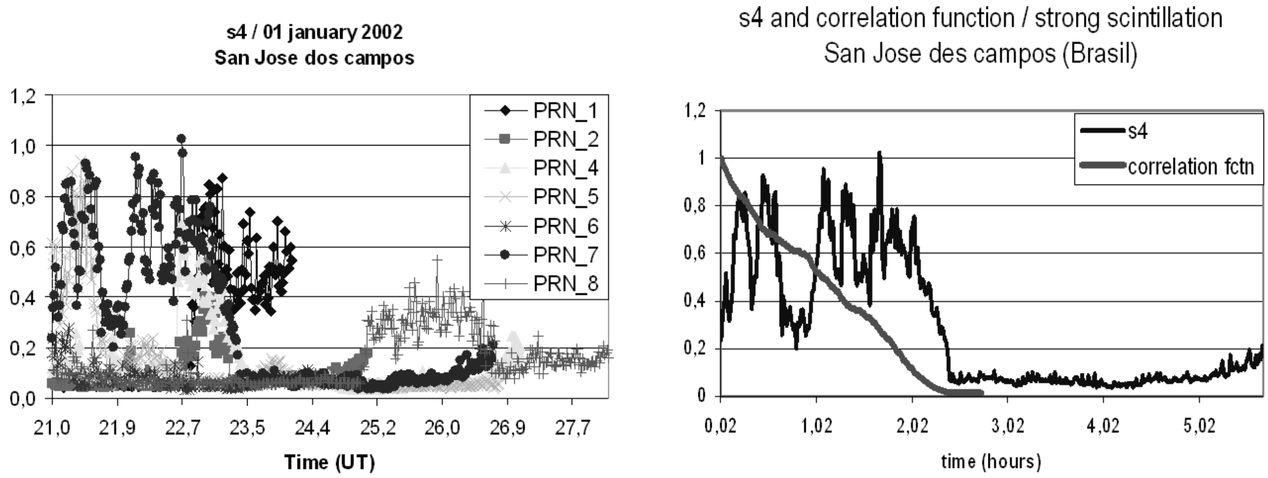

Figure 7: S4 recorded for each satellite visible on 2002-01-01 and correlation function

4. Probability of simultaneous fading

Figure 8 presents the probability of simultaneous fading, given the value of S4 and given the number of satellites affected. This probability drops quickly with the number of satellites affected and increases with the flux number. All satellites were used for this calculation.

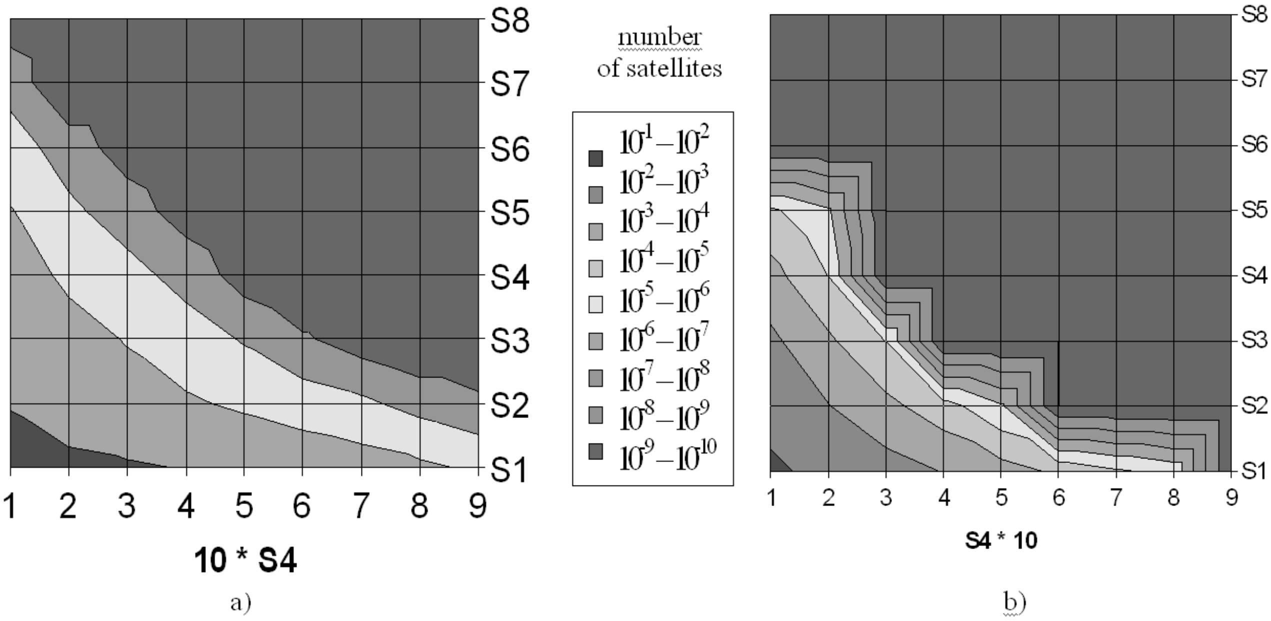

Figure 8: Probability of simultaneous fading (log scale). The left plot corresponds to the data recorded in Douala with a flux number equal to 100. The right plot corresponds to the data recorded in São Jose dos Campos with a flux number equal to 190. The vertical scale is the number of satellites simultaneously affected from 1 to 8.

5. Local time dependency

One of the advantages of the geostationary satellite observed from Douala is its fixed geometry. This allows the analysis of the temporal variation in the scintillation behavior. Figure 9 presents the amplitude scintillation recorded during a whole day. As expected from the results of other measurements campaigns, scintillation occurs only during nighttime, essentially during the post sunset period between 19 and 24 LT.

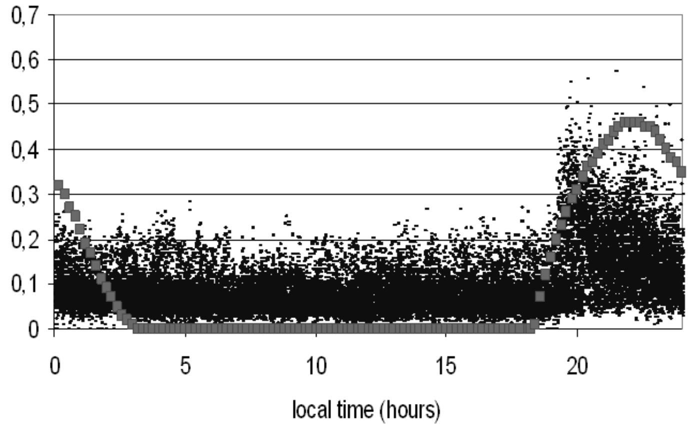

Figure 9: S4 vs. local time for the GEO satellite during the first 20 days of measurements compared with GISM prediction (red squares)

6. Seasonal dependency

An analysis of the long term temporal variation of scintillation has been done with the data recorded in Douala. The mean value of S4 over the nighttime period is chosen as an indicator of the scintillation activity for a particular day. Figure 10 presents the evolution of this parameter over the 150 days of observation. It appears that after June the scintillation activity seems to be quieter. The same observation was made in South America.

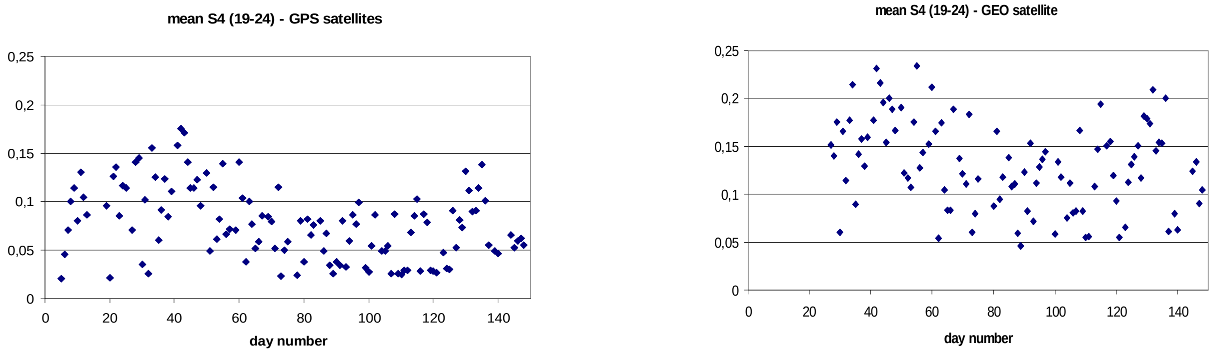

a) b)

Figure 10: mean value of S4 calculated from the S4 values of all GPS satellites with elevation angles greater than 30° over the nighttime period (a) and for the GEO satellite (b).

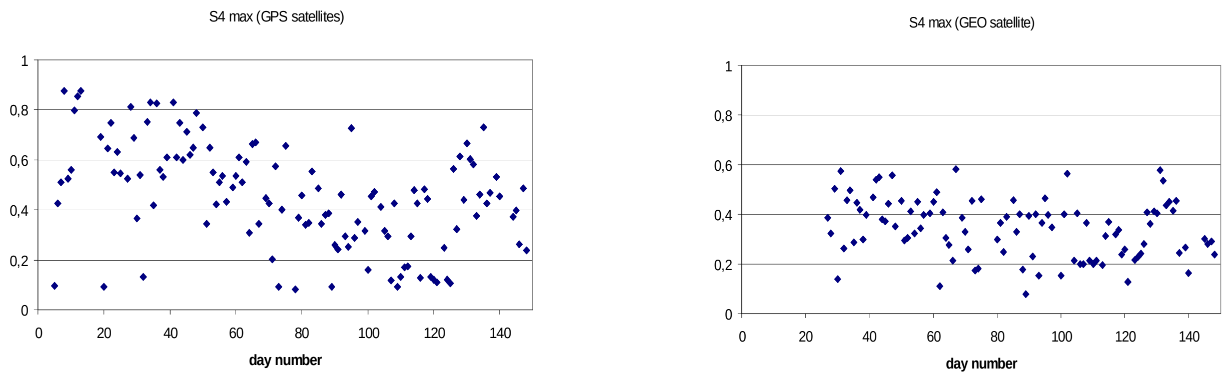

a) b)

Figure 11: highest values recorded one day for S4 on all the links of the GPS constellation for the nighttime period (a) and for the GEO satellite (b).

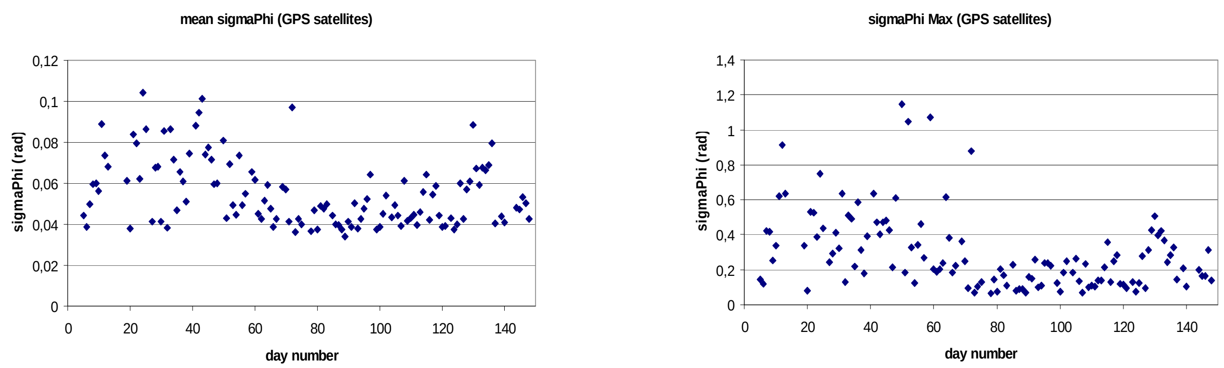

Figure 12: mean and highest values recorded one day for σ_ϕ on all the links of the GPS constellation.

Figures 11 presents the highest values obtained each day for the worst link for the GPS and the GEO satellites. In the case of the GEO, due to the fact that the C/N value is lower (cf figure 16), loss of locks occur for lower values of S4 than for the GPS. This is the reason why the values recorded for the GEO are lower than for the GPS links. In all cases, S4 has been calculated on 1 mn samples. The mean and max values over all GPS links are presented on figure 10. The peak values for sigma phi in radians are in the same range than S4. The phase was not measured for the GEO.

7. Loss of lock

The receiver provides the lock time. This value indicates how long the receiver has been locked to the carrier phase of the GPS signal. This also indicates the time of the last loss of lock and it can be used to detect this failure.

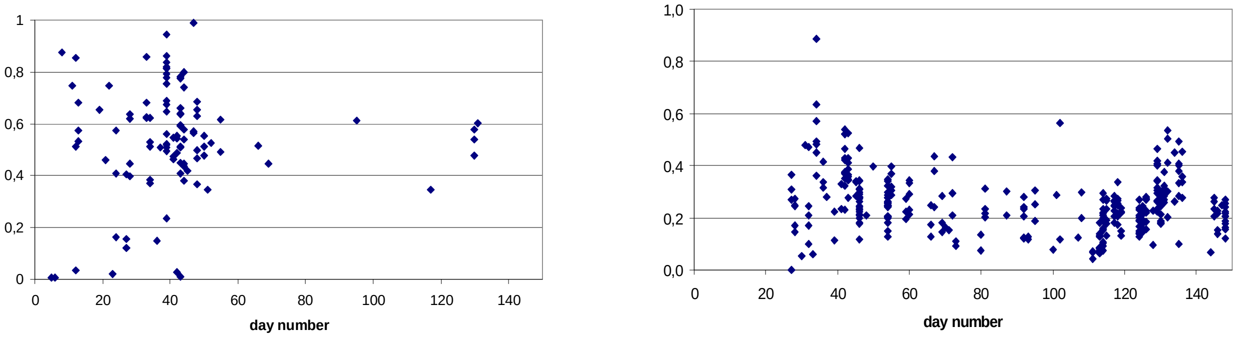

a) b)

Figure 13: S4 before loss of lock of L1 carrier for all GPS satellites over 30° (a) and for the GEO (b). For each day, there may have several losses of lock. Only nighttime (19-24 LT) losses of lock were considered. The difference of S4 levels for GPS and GEO satellite is related to the signal level, which is significantly lower for the GEO.

The GEO link uses a GPS like signal with an L1 carrier. That is the reason why we have only considered the loss of lock of L1. Figure 13 presents the value of S4 before the loss of lock. It is possible to estimate the probability of having a loss of lock and a given value of S4. In addition, the frequency of occurrence of S4 may also be evaluated from the samples. Therefore we can calculate the probability of loss of lock vs. the value of S4. This result is presented on Figure 14.

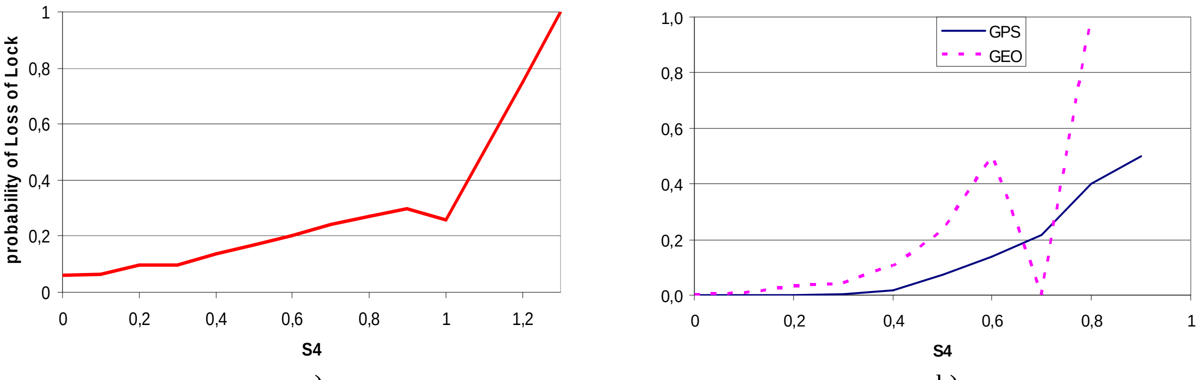

a) b)

Figure 14: Probability of loss of lock, given the value of S4 in São Jose dos Campos (a) and Douala (b). For the GEO, for S4 greater than 0.6, there are not enough loss of lock occurrences to get correct statistics. This explains the discontinuity in the curve.

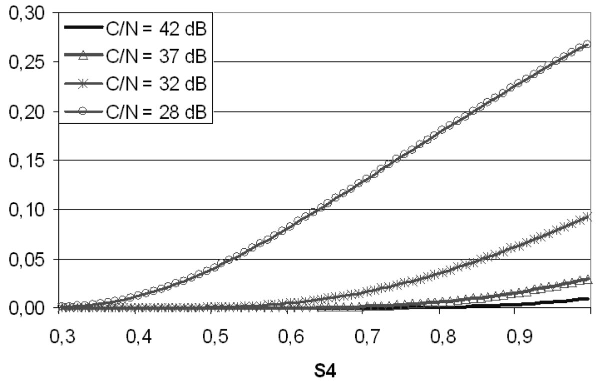

Figure 15: Probability of Loss of Lock for a typical receiver obtained with GISM scintillation model

As a comparison, the Figure 15 presents the values obtained with GISM for a typical receiver. The same behaviour is exhibited. The differences of levels are related to different values of the receiver parameters and to the fact that curves presented on figure 13 have plotted independently of the value of C/N and correspond consequently to an average value of this ratio. The GISM model allows setting any value to these parameters.

In the GISM model, loss of lock is evaluated through the standard thermal noise tracking error for the PLL [4]:

$$\sigma_{\Phi T}^2 = \frac{B_n}{(c/n_0)\ Is}\left[1 + \frac{1}{2\eta(c/n_0)\ Is}\right]$$

where Bn is the receiver bandwidth, and η is the predetection time. For airborne GPS receiver, Bn = 10 Hz and η = 10 ms. Is is the scintillation intensity. Its mean value is 1 and it has a Nakagami distribution characterized by S4.

This relation expresses the thermal noise as a decreasing function of the scintillation intensity. As a result, if $\sigma_{\Phi T}$ is above the 15° threshold then Is is below a value computed using this relation. As Is distribution is known for a given S4, the probability of occurrence of "Is < threshold" can be evaluated. The result is the probability of Loss of Lock. Figure 14 presents this probability versus S4 at given values of the C/N0. It can be noticed that links with high C/N0 are quite robust. On the contrary, links with low values of C/N0 are likely to be lost.

There are more losses of lock on the GEO link than on the GPS links (Figure 13). For the SBAS signal, the loss of lock appears at a lower value of S4. This is due to the lower signal power provided by the GEO satellite. The receiver also provides the C/N0 value of the link. As can be noticed on Figure 16, the C/N0 value is 10 dB lower for the GEO satellite link.

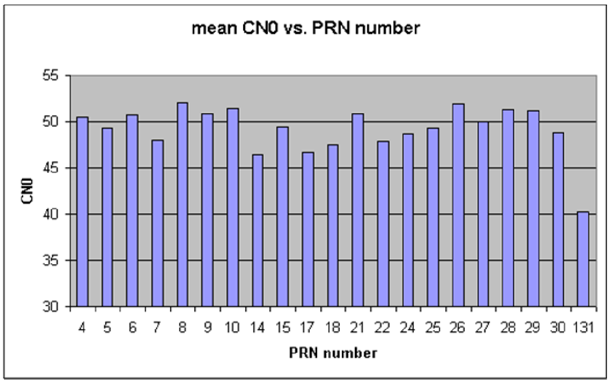

Figure 16: mean C/N0 for each satellite PRN number. PRN 131 corresponds to the GEO satellite. The GPS satellites taken into account are all seen with an elevation angle greater than 30°. The elevation angle for the GEO satellite is 28°.

The frequency of occurrence of S4 is presented on Figure 17 for the two data sets. It exhibits a Log normal distribution. The red line (Sao Jose dos Campos) and dashed line (GEO satellite) have been plotted with a reduced data set on the contrary to the blue curve (GPS satellites in Douala).

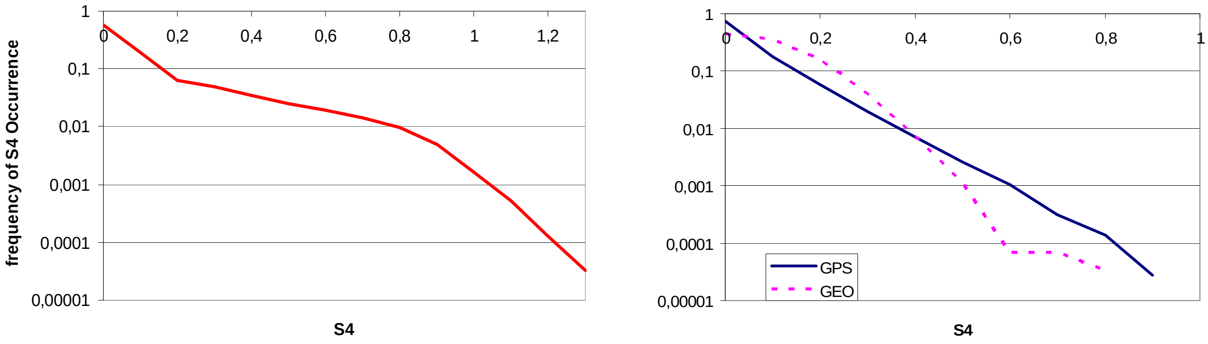

Figure 17: Frequency of occurrence of S4 in São Jose dos Campos (a) and Douala (b). Ten S4 intervals of equal width were considered. Each sample is counted in one of these intervals.

7. Positioning error

The receiver used for this study is unable to record the position. To analyze the effect of scintillation on the positioning error, we have to simulate the receiver behavior affected by scintillation characterized by S4. According to [4], in presence of scintillation, the tracking variance for a DLL (in C/A code chips squared) may be expressed as :

$$\sigma_\tau^2 = \frac{B_n\, d}{2\,(c/n_0)\,(1-S_4^2)}\left[1+\frac{1}{\eta\,(c/n_0)\,(1-2\,S_4^2)}\right]$$

Where Bn is the one-sided noise bandwidth (typical value is 0.1 Hz) and d is the correlator spacing in C/A code chips (typical value is 1 to 0.1). η is the predetection time. The chip length is about 293 m.

To evaluate the positioning error, the following steps were performed for each tracked satellite:

- S4 is measured.
- σ_τ is deduced from S4.
- assuming a gaussian distribution characterized by σ_τ, a range error is computed.
- a Yuma file is used to evaluate the satellite position in order to fill the navigation equations.

The navigation equations are solved with these range errors to compute a positioning error.

Figure 18 presents the results of this simulation. In that example, the scintillation effects aren't significant. The mean value of S4 shows that the scintillation activity was weak. As a result, the number of tracked satellites was always high enough to mitigate the range error.

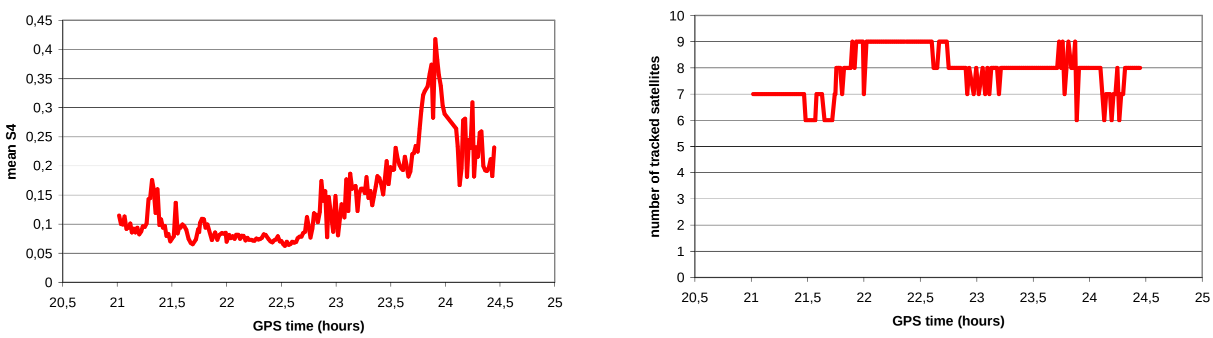

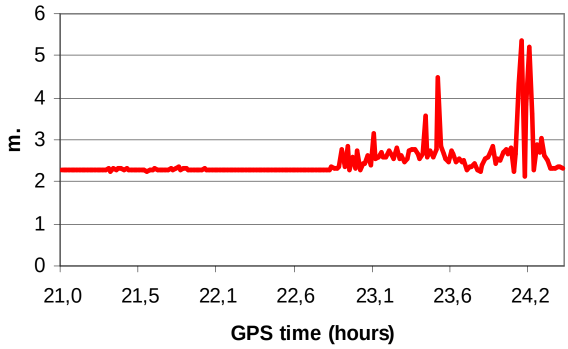

Figure 18: The first curve represents the mean value of S4 (all visible GPS satellites), it shows the scintillation activity. The second presents the number of tracked satellites. The last one corresponds to the evaluated positioning error.

9. Conclusion

The characteristics of signal scintillations, due to the propagation through ionosphere inhomogeneities, have been presented. This as been illustrated by measurement results of two measurements campaigns: in Douala, Cameroon starting beginning of year 2004 with an average solar flux number equal to 110 and in Sao Jose dos Campos, Brazil, during the first two weeks of January 2002 with a solar flux number equal to 190.

One interesting feature of the measurement campaign in Douala was the fact that we had an additional link with a GEO satellite. This link is not moving with respect to the ground station and is therefore only affected by the motion of the ionosphere. It is seen from the observation point with an elevation angle equal to 28° which is in principal large enough to get rid of multipath effects.

Results have been presented for the local time dependency, the probability of loss of lock, the positioning error due to scintillations, the S4 distribution, the spatial extent and the probability of the simultaneous loss of lock.

The measurements show the usual dependency to local time: the scintillations appear at post sunset hours and may last a few hours. Modeling with GISM model provides concurrently a reasonable agreement. The probability of loss of lock has been calculated, but for an average value of C/N. This point should be investigated in more detail in the future but a rough estimate has been obtained. The simultaneous probability of loss of lock, which highly depends on the solar flux number has also been estimated.

The positioning error has been calculated for a case of medium values of the scintillation ratio. The errors obtained are a few meters in that case. It increases very rapidly with S4.

We have shown that the S4 probability seems to converge towards a log normal distribution. Three curves have been plotted (GEO satellite, GPS low latitudes in Brazil and GPS low latitudes in Africa) and increasing the data base shows this tendency. Finally we have calculated the spatial extent of the inhomogeneities region, depending on the solar flux number. Values of hundreds of km have been estimated.

Another measurement campaign in the frame of the ESA / ESTEC PRIS project (Prediction of Ionospheric Scintillation) is currently running on a larger basis, with receivers all over the globe. This will allow to enlarge the data base which has been initiated.

References

[1] Y. Beniguel, “Global Ionospheric Propagation Model (GIM): a propagation model for scintillations of transmitted signals”, *Radio Sci*ence, Vol 37, N° 3, May 2002.

[2] A.J. Van Dierendonck, B. Arbesser-Rastburg “Measuring Ionospheric Scintillation In The Equatorial Region Over Africa, Including Measurements From Sbas Geostationary Satellite Signals”, Beacon Symposium, Trieste, Italy, October 2004.

[3] J-P Adam, Y. Béniguel, E. De Paula, B. Arbesser-Rastburg “Analysis of scintillation data recorded at low latitudes” to appear in *Radio Science*

[4] Conker, R. S., M. B. El-Arini, C. J. Hegarty, T. Hsiao, "Modeling the Effects of Ionospheric Scintillation on GPS/SBAS Availability", *Radio Science*, January/February 2003.